

21. ASH LAYERS, HYALOCLASTITE, AND ALTERATION OF BASALTIC GLASS, LEG 65¹

Hans-Ulrich Schmincke, Institut für Mineralogie, Ruhr-Universität, D-4630 Bochum, Federal Republic of Germany

ABSTRACT

Three types of tephra deposits were recovered on Leg 65 of the Deep Sea Drilling Project (DSDP) from three drill sites at the mouth of the Gulf of California: (1) a series of white ash layers at Sites 483, 484, and 485; (2) a layer of plagioclase-phyric sideromelane shards at Site 483; and (3) an indurated, cross-bedded hyaloclastite in Hole 483B.

The ash layers in (1) are composed of colorless, fresh rhyolitic glass shards with minor dacitic and rare basaltic shards. These are thought to be derived from explosive volcanoes on the Mexican mainland.

Most of the shards in (2) are fresh, but some show marginal to complete alteration to palagonite. The composition of the glass is that of a MORB-type tholeiite, low in Fe and moderately high in Ti, and possibly erupted from off-axis seamounts. Basaltic glass shards occurring in silt about 45 meters above the basement at Site 484A in the Tamayo Fracture Zone show a distinctly alkalic composition similar to that of the single basement basalt specimen drilled at this site.

The hyaloclastite in (3) is made up chiefly of angular sideromelane shards altered to smectite and zeolites (mainly phillipsite) and minor admixtures of terrigenous silt. A very high K and Ba content indicates significant uptake of at least these elements from seawater. Nevertheless, the unusual chemical composition of the underlying massive basalt flow is believed to be reflected in that of the hyaloclastite. This is a powerful argument for interpreting the massive basalt as a surface flow rather than an intrusion.

Glass alteration is different in the glassy margins of flows than in thicker glassy pillow rinds. Also, it appears to proceed faster in coarse- than fine-grained sediments.

INTRODUCTION

Between January and March, 1979, the *Glomar Challenger* drilled six major holes at the mouth of the Gulf of California in order to study crustal accretion processes occurring during the early stages of the formation of an oceanic rift system (Fig. 1) (Robinson et al., this volume). The sediment cover on top of the basalts ranges from 50 to 150 meters, and up to 160 meters of basalt was drilled in the deepest hole. One of the surprising discoveries of the leg was the abundance of sediments found interlayered with the basalts (Rangin et al., this volume).

The purpose of this chapter is to describe briefly the textures and chemical composition of some volcanic sediments encountered above basement as well as in the sediments interlayered with the basalts. Some chemical analyses of nonvolcanic sediments are also reported, and the alteration of the basaltic glass is briefly discussed. The petrography, mineralogy, and chemistry of the basalts are discussed in two companion chapters (Griffin et al., and Flower et al., this volume).

METHODS

High-precision refractive indices of shards were measured using the method described in Schmincke (1981). Microprobe analyses were made using a wide defocussed beam and an automated CAMEBAX microprobe. The analyses reported are averages of up to six analyses. The methods used for the bulk chemical analyses are described in Flower et al. (this volume).

ASH LAYERS

White vitric ash occurs in pods and thin deformed layers (<2 cm thick) within the sediments overlying the

basement in Holes 483 and 483C, which are 100 meters apart. In Hole 483 the ash occurs chiefly in Section 6-2, about 41 meters below the mudline and 75 meters above basement. The sediment is a muddy siliceous nannofossil ooze. In Hole 483C, ash also occurs in pods about 40 to 45 meters below the mudline at a similar depth above basement. Because of the similarity in depth and the proximity of the holes, the ash is considered to be stratigraphically equivalent in both holes. The fact that relatively pure white ash occurs in pods (Fig. 2) might result from the disturbance of one or more ash layers by drilling. In Hole 484A, minor ash occurs in Core 1 about 8 meters below the mudline and 47 meters above the basement. Small amounts of ash also occur at Site 485 about 8 meters and 45 meters below the mudline.

The shards recovered are mostly fine ash size (<125 μm) and the bulk of the ashes show a restricted range in composition. The refractive index ranges mostly between 1.5004 and 1.502, indicating a rhyolitic composition (Table 1). A minor amount of rhyodacitic ash was found in all of the samples from Hole 483C except for Sample 483C-1-2, 0-3 cm, which displays an index ranging from about 1.50 to 1.57, corresponding to a range in composition from rhyolite to basaltic andesite (Fig. 3). Light-brown and brown shards fall in the range of refractive indices (and thus chemical compositions) delineated by Schmincke (1981) as colorless ($n < \sim 1.53$), light brown ($n \sim 1.53-1.56$), and brown ($n > \sim 1.56$). The compositions of the shards in Hole 483C are identical, but the rhyolite shards in Hole 485 are highly fractionated (Table 2). The oxide totals are between about 94% and 96%; it is thus not certain whether or not the dominance of Na over K in the samples from Hole 483C and that of K over Na in Hole 485 is significant.

Likely sources for these ash falls are young volcanoes along the nearby Mexican coast. The island of Socorro,

¹ Lewis, B. T. R., Robinson, P., et al., *Init. Repts. DSDP*, 65: Washington (U.S. Govt. Printing Office).

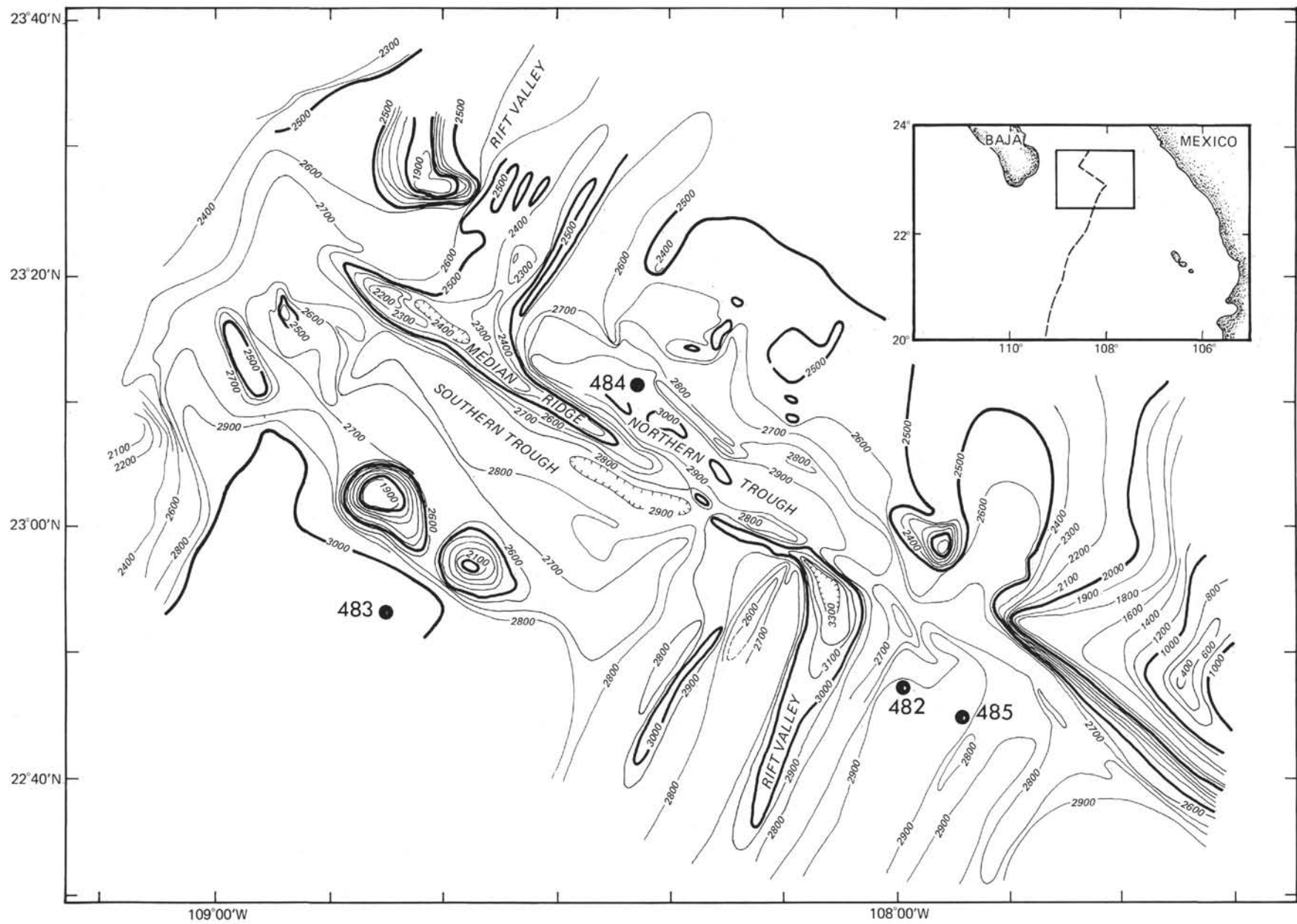


Figure 1. Location of sites drilled on Leg 65 (depths shown in corrected m).

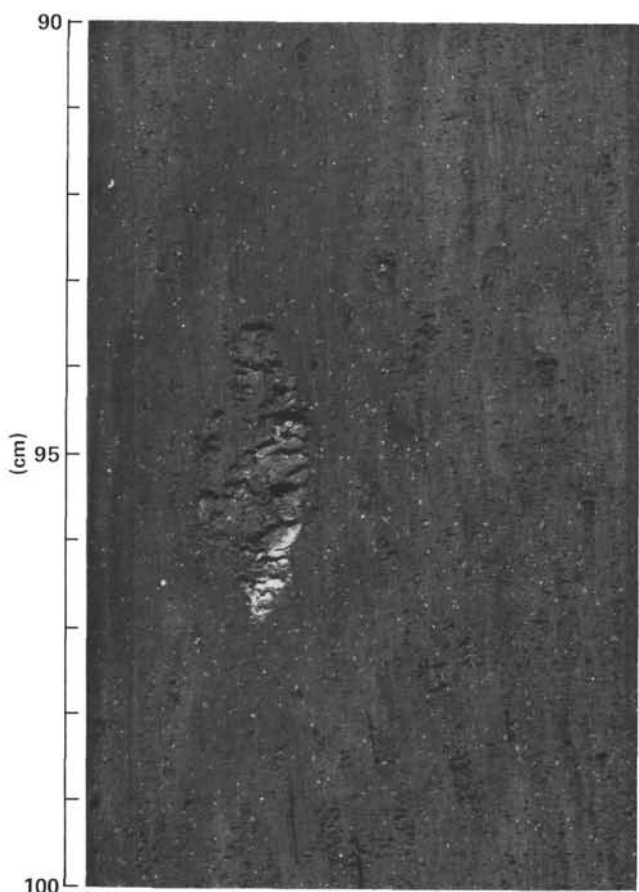


Figure 2. Ash patch (3 cm long) in a matrix of soft, vitric silty clay; Sample 483C-1-3, 90–100 cm.

about 50 km southwest of the area, is a less likely source because it is probably too far away to produce centimeter-thick ash layers and because the rhyolites from Socorro and the other Revillagigedo Islands are peralkaline in composition (Bryan, 1966). Even though the alkali values reported here may have been modified by diagenesis, the low Fe, Ti, and Al contents identify the shards as calc-alkaline rather than peralkaline. The number of ash layers is not high, possibly because of the high sedimentation rate and the general mode of deposition by mass flow (Rangin et al., this volume).

BASALTIC SHARDS

Basaltic shards occur in trace amounts in several rhyolitic ash layers and make up all of the volcanic clasts in Section 483-7-2 (Plate 1; Figs. 1, 2; see also Fig. 3 and Tables 1, 2). They are nonvesicular, blocky to cuneiform, and sliverlike. Their basaltic composition is shown by their brown color, low refractive index (about 1.60), and chemical composition. The composition of the sideromelane shards from Hole 484A and Site 485 represents moderately evolved, high Ti, MORB-type basalts, with the shards from Hole 484A being significantly richer in Ti, K, and P. The basalt from this site, which is situated in the Tamayo Fracture Zone, is also distinctly more alkalic (Flower et al., this volume). The shards from the hyaloclastite layers are quite mafic (Mg No. =

61.4) but have a moderately high Ti content. All of the basaltic shards are believed to be derived from glassy crusts which have spalled off extrusive pillow or sheet-flow lavas. The sporadic shards in samples from Sites 484 and 485 are interpreted as accidental admixtures into a rhyolite fallout layer. The origin of the sideromelane shard layer at Site 483 may be connected with a nearby off-axis eruption producing plagioclase-phyric, MORB-type basalts, possibly on one of the two nearby seamounts shown in Figure 1. The exact mode of origin of these shards is unknown, but thermal contraction of glassy rinds followed by dispersal by bottom currents or eruption-induced convection is most likely. Similar layers of nonvesicular sideromelane shards are not uncommon and have been observed both in sediments overlying the basement (Scheidegger, 1973) and interbedded with pillow flows (Schminke et al., 1978) and will be discussed in more detail with reference to Leg 70 (Schminke, in press).

INDURATED HYALOCLASTITE

Pillow breccias are unusually sparse in the basaltic series encountered on Leg 65. A 5-cm-thick, indurated hyaloclastite layer was found on top of a massive flow (Fig. 4). It is medium grained and composed of about 90% angular, nonvesicular shards and minor nonvolcanic sand and biogenic debris. All of the shards are completely altered, chiefly to smectite, with a series of concentric bands (of a Ti-bearing phase?) showing former successive stages of palagonitization (Plate 1, Fig. 3). Some shards have been partly dissolved and are represented by a network of smectite veins, probably representing the initial stages of palagonitization along cracks. A number of plagioclase and detrital quartz grains are also partially dissolved (Plate 1, Fig. 3). The original pore spaces between grains and pores resulting from the dissolution of clasts are partially filled with zeolites, chiefly phillipsite.

Chemically, the hyaloclastite is clearly derived from a sideromelane ash layer of the type previously described (Table 3). The low Ti and Fe and high Al and Mg concentrations in this rock may reflect the composition of the underlying basalt (Flower et al., this volume). However, the composition has been modified by admixtures of nonvolcanic components and by interaction with seawater as will be discussed.

ALTERATION OF GLASS

The alteration of sideromelane in the holes drilled on Leg 65 shows clear differences in degree and time. Most of the glass from pillow margins is fresh but shows alteration to "gel-palagonite" along fractures, vesicle walls, and some crystal boundaries, i.e., surfaces accessible to water (Table 4). The marginal alteration of sideromelane shards in Sample 483-7-2 is of this type (Plate 1).

More pervasive alteration is shown by the thinner, former glass rinds of sheet flows, which rarely have fresh glass preserved (Griffin et al., this volume). Instead, the glass is represented by darker brown "altered glass" lacking gel palagonite-type banding but sometimes showing faint birefringence without "fibro palagonite" textures.

Table 1. Abundance, refractive indices, color, and shape of glass shards in ash layers from Sites 483, 484, and 485.

Sample (interval in cm)	Sample Weight (g)	Insoluble Residue (g)	Organic and Carbonaceous Materials (wt. %)	Glass in 63–125 μm Size Range (%)	Refractive Index, n	Relative Abundance of Shard Type (%)
Hole 483						
6-2, 38-31	—	—	—	100	1.5014 \pm 0.0003	tp, spl
7-2, 11-16	5.91	3.80	41.8	~10	1.5973 \pm 0.0006	bw, spl
Hole 483C						
1-1, 49-51	3.97	2.88	27.5	80	1.5009 \pm 0.0007	bj, bw, rb, spl
1-1, 124-129	8.03	5.83	27.4	80	1.5250 \pm 0.0003	bw, rb, bj
1-1, 124-129	2.53	2.34	7.5	95	1.5010 \pm 0.0003	bj, bw, rb
1-2, 0-3	1.83	1.34	26.8	50	1.5004 \pm 0.0003	bj, bw, rb, tp
					1.5271 \pm 0.0003	rb, spl
					1.5008 \pm 0.0003	bj, bw, tp
					1.5233 \pm 0.0004	bj, tp, bw
					1.5375 \pm 0.0004	rb, spl; l-brown
					1.5625 \pm 0.0004	rb, spl; brown
1-2, 69-75	6.90	4.79	30.6	20	1.5014 \pm 0.0005	bw, bj, tp
1-3, 92-96	5.72	4.40	23.1	70	1.5237 \pm 0.0003	rb
					1.5014 \pm 0.0005	bj, bw, tp
					1.5248 \pm 0.0003	spl, rb
Hole 484A						
1-5, 101-103	7.16	2.56	64.2	5	1.5004 \pm 0.0002	spl
Hole 485						
2-2, 38-40	6.18	5.19	16.0	10	1.5005 \pm 0.0003	bw, spl
6-3, 13-15	6.33	4.88	22.9	10	1.4991 \pm 0.0002	bw, spl
					1.5020 \pm 0.0005	spl
						100

Note: tp = tubular pumice; spl = spallation shard; bw = bubble wall shard; bj = bubble function shard; rb = round bubbles.

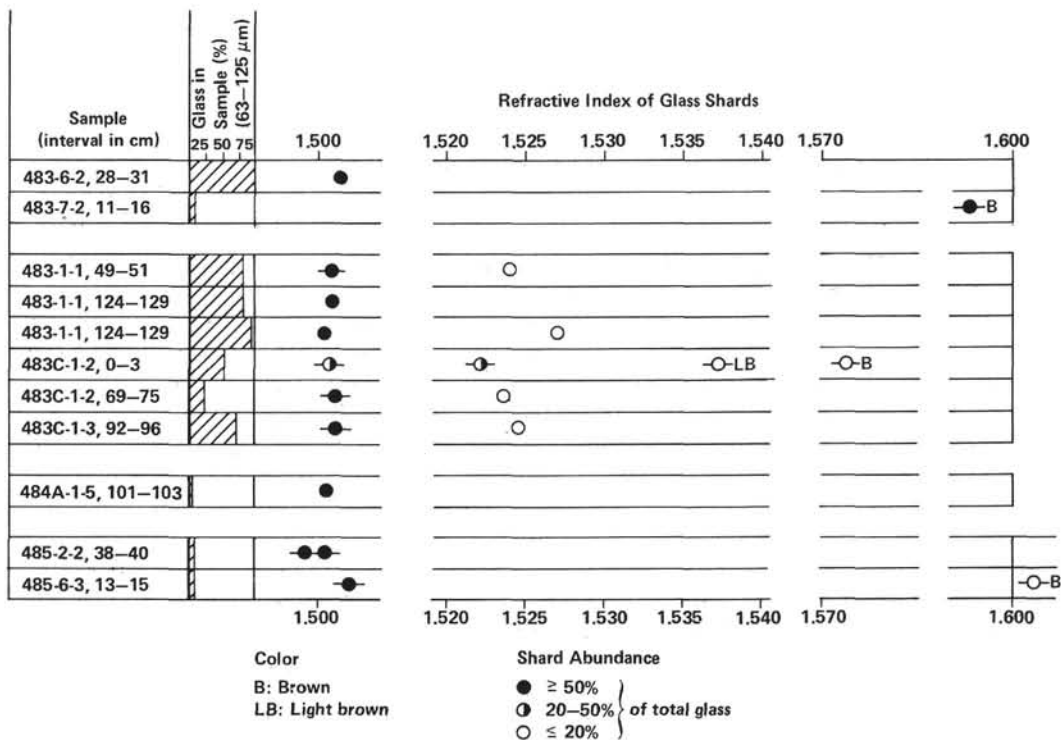


Figure 3. Stratigraphic distribution, abundance, color, and range of refractive indices of glass shards of main ash layers encountered during Leg 65.

A similar type of pervasive alteration in Sample 483B-26-1 shows islands of fresh light-brown sideromelane, surrounded by transparent rims with a gradational inner but sharp outer interface toward a deeper brown outer zone that becomes lighter colored toward the original fracture or outer surface diffusion front (Plate 1, Fig.

4). Chemical analyses of fresh sideromelane and colorless and brown alteration zones from two samples show pronounced differences in element migration with alteration (Table 4). Sample 483-30-3 shows a decrease in Ca by a factor of 4 and of Na by a factor of 2.5, with a gain in K by a factor of 10. Slight relative enrichments are

Table 2. Chemical composition of rhyolitic and basaltic shards from ash layers at Sites 483, 484, and 485.

	Sample						
	483-7-2, 11-16 cm Shard	483C-1-1, 49-51 cm Shard	483C-1-2, 0-3 cm Shard	484A-1-5, 101-103 cm Shard	n.d.	485-2-2, 38-40 cm Shard	485-6-3, 13-15 cm Shard
Refractive Index	1.5973	1.5009	1.5008		1.4991		1.606
SiO ₂	50.87 (51.19)	72.77 (76.61)	72.29 (77.08)	50.17 (51.02)	74.16 (77.42)	50.82 (51.58)	
TiO ₂	1.62 (1.63)	0.12 (0.12)	0.07 (0.07)	2.67 (2.72)	0.05 (0.05)	2.38 (2.42)	
Al ₂ O ₃	14.65 (14.74)	13.16 (13.85)	12.72 (13.57)	13.68 (13.91)	11.95 (12.48)	13.18 (13.38)	
FeO* ^a	9.64 (9.70)	0.79 (0.83)	0.82 (0.88)	11.59 (11.79)	0.84 (0.88)	11.83 (12.01)	
MnO	0.15 (0.15)	0.06 (0.06)	0.05 (0.05)	0.17 (0.17)	0.04 (0.04)	0.31 (0.31)	
MgO	7.49 (7.54)	0.13 (0.13)	0.16 (0.17)	6.58 (6.69)	0.05 (0.05)	6.55 (6.65)	
CaO	11.64 (11.71)	0.71 (0.75)	0.66 (0.70)	9.64 (9.80)	0.35 (0.37)	10.29 (10.44)	
Na ₂ O	3.09 (3.11)	4.06 (4.27)	3.87 (4.13)	3.33 (3.39)	3.69 (3.85)	2.89 (2.93)	
K ₂ O	0.09 (0.09)	3.18 (3.35)	3.04 (3.24)	0.25 (0.25)	4.64 (4.84)	0.08 (0.08)	
P ₂ O ₅	0.14 (0.14)	0.01 (0.01)	0.02 (0.02)	0.26 (0.26)	0.02 (0.02)	0.19 (0.19)	
Total	99.38 (100.00)	94.99 (100.00)	93.71 (100.00)	98.34 (100.00)	95.79 (100.00)	98.52 (100.00)	
Mg No.	61.43	25.22	28.57	53.78	10.87	53.16	

Note: Values given in wt.%; recalculated values are given in parentheses.

^a FeO* = Total Fe as FeO.



Figure 4. Indurated (palagonitized) bedded tuff, Sample 483B-8-1, 21-28 cm. (See Fig. 1 of plate for photomicrograph of tuff.)

Table 3. Bulk chemical composition of indurated hyaloclastite from Site 483 and nonvolcanic marls and sandstones from Site 485.

Hyaloclastite	Sample			
	483B-8-1, 24–27 cm	485A-23-1, 42–44 cm	485A-38-1, 84–86 cm	485A-38-1, 96–98 cm
SiO ₂	50.3 (55.0)	30.8 (60.1)	58.3 (66.7)	60.7 (68.2)
TiO ₂	0.86 (0.94)	0.45 (0.88)	0.66 (0.75)	0.69 (0.76)
Al ₂ O ₃	16.01 (17.49)	8.42 (16.44)	15.62 (17.86)	15.93 (17.90)
Fe ₂ O ₃	4.02 (4.39)	1.51 (2.95)	2.77 (3.17)	1.43 (1.61)
FeO	3.73 (4.08)	2.68 (5.23)	0.96 (1.10)	0.91 (1.02)
MnO	0.30 (0.33)	0.26 (0.51)	0.06 (0.07)	0.05 (0.06)
MgO	9.25 (10.11)	1.97 (3.85)	2.62 (1.06)	2.76 (0.91)
CaO	2.48 (1.96)	26.91 (1.31)	2.64 (0.00)	1.32 (0.00)
Na ₂ O	3.25 (3.55)	3.85 (7.51)	3.90 (4.46)	4.00 (4.94)
K ₂ O	1.55 (1.69)	0.24 (0.47)	3.73 (4.27)	3.78 (4.25)
P ₂ O ₅	0.07 (0.08)	0.11 (0.21)	0.16 (0.18)	0.15 (0.17)
H ₂ O ⁺	7.52	0.79	4.43	5.39
CO ₂	0.54	20.59	3.92	3.17
C	—	—	0.70	0.65
Total	99.88 (100.00)	98.58 (100.00)	100.47 (100.00)	100.93 (100.00)
Mg No.	72.07	—	—	—
S	0.33 (0.36)	0.33 (0.64)	0.05 (0.06)	0.05 (0.06)
Cl	0.15 (0.16)	0.06 (0.12)	0.24 (0.27)	0.15 (0.17)
O/S, Cl	0.20 (0.22)	0.18 (0.35)	0.08 (0.09)	0.06 (0.07)
Cr	237 (259)	33 (64)	47 (54)	49 (55)
Ni	38 (42)	21 (41)	21 (24)	24 (27)
Cu	64 (70)	14 (27)	17 (19)	29 (33)
Zn	72 (79)	42 (83)	59 (67)	78 (88)
Rb	36 (39)	2 (4)	111 (127)	114 (128)
Sr	126 (138)	233 (455)	165 (189)	162 (182)
Y	26 (28)	25 (49)	29 (33)	26 (29)
Zr	128 (140)	133 (260)	194 (222)	200 (224)
Nb	9 (10)	12 (23)	19 (22)	20 (22)
Ba	450 (492)	100 (195)	700 (801)	640 (719)

Note: Values recalculated on an H₂O – and CO₂ – free basis are given in parentheses.

Table 4. Composition of fresh and altered glass from a pillow margin (Section 483B-30-3) and the base of a massive flow (Section 483B-26-1).

483B-30-3, 18–22 cm	Sample				
	483B-30-3, 18–22 cm	483B-26-1, 39–40 cm	483B-26-1, 39–40 cm	483B-26-1, 39–40 cm	Dark Brown Outer Zone
	Fresh Glass	Altered Glass	Fresh Glass	Colorless Rim	
SiO ₂	50.78 (51.34)	45.42 (52.53)	51.35	38.1 (44.17)	43.80 (46.18)
TiO ₂	1.80 (1.82)	1.44 (1.67)	2.21	2.78 (3.22)	2.54 (2.68)
Al ₂ O ₃	13.97 (14.13)	14.84 (17.16)	13.93	10.30 (11.94)	12.84 (13.54)
FeO ^a	10.49 (10.61)	12.27 (14.19)	11.40	12.89 (14.94)	13.41 (14.16)
MnO	0.20 (0.21)	0.12 (0.13)	0.22	0.32 (0.37)	0.27 (0.28)
MgO	7.27 (7.35)	7.80 (9.02)	7.03	8.57 (9.85)	8.63 (9.10)
CaO	11.34 (11.44)	2.51 (2.90)	10.97	12.59 (14.60)	12.55 (13.23)
Na ₂ O	2.77 (2.80)	0.92 (1.06)	2.62	0.49 (0.57)	0.41 (0.43)
K ₂ O	0.11 (0.11)	0.89 (1.03)	0.11	0.06 (0.06)	0.17 (0.17)
P ₂ O ₅	0.16 (0.16)	0.25 (0.30)	0.23	0.17 (0.20)	0.23 (0.23)
Total	98.90 (100.00)	86.46 (100.00)	100.08	86.26 (100.00)	94.85 (100.00)
Mg No.	58.69	56.58	55.83	57.68	56.88

Note: Values given in wt.%; recalculated values are given in parentheses.

^a FeO* = total Fe as FeO.

also shown for Al, Fe, and Mg. Sample 483-26-1 varies insignificantly except for a drastic loss of Na by a factor of 5, slight gains in Ti, Fe, Mg, and Ca, and a slight loss in Al. The most striking differences from Sample 483-30-3 are the increase in Ca and the relatively small gain in K. The reasons for these contrasting types of alteration are not known.

Elemental changes resulting from diagenetic alteration are more difficult to evaluate in hyaloclastite Sample 483B-8-1, because of the admixture of nonvolcanic clasts noted above (Table 3). However, the changes observed are similar to those in Sample 483-30-3, which is more representative of the changes commonly observed during palagonitization. Most pronounced is the gain in K among the major elements and in Rb and Ba among the trace elements resulting from uptake from seawater. A major decrease in concentration is shown by Ca. The high concentrations of the compatible trace elements Cr and, to a lesser degree, Ni also reflect the former basaltic composition of most of the clasts. Since elements such as Ti, Fe, and Al are relatively stable, the bulk composition of this altered rock shows less pronounced elemental redistribution than the palagonite reported in Table 4. Thus, the composition of the hyaloclastite may reflect that of the underlying basalt, indicating that the glass shards were derived from the top of the massive basalt. This is a major argument for interpreting the massive basalt as an extrusive lava flow rather than an intrusion.

ACKNOWLEDGMENTS

This work was supported financially by the Deutsche Forschungsgemeinschaft. I am grateful to M. Simon for measuring the refractive indices and to M. Becker for help with the microprobe.

REFERENCES

- Bryan, W. B., 1966. History and mechanism of eruption of soda-rhyolite and alkali basalt: Socorro Island, Mexico. *Bull. Volcanol.* 29: 453–479.
- Scheidegger, K. F., 1973. Volcanic ash layers in deep sea sediments and their petrological significance. *Earth Planet. Sci. Lett.*, 17: 397–407.
- Schmincke, H.-U., 1981. Ash from vitric muds in deep sea cores from the Mariana Trough and fore-arc region (South Philippine Sea) (Sites 453, 454, 455, 458, 459 and SP), Deep Sea Drilling Project, Leg 60. In Hussong, D. M., Uyeda, S., et al., *Init. Repts. DSDP*, 60: Washington (U.S. Govt. Printing Office).
- _____, in press. Ryolitic and basaltic ashes from the Galapagos Spreading Center. In Honnorez, J., and Von Herzen, R. P., et al., *Init. Repts. DSDP*, 70: Washington (U.S. Govt. Printing Office).
- Schmincke, H.-U., Robinson, P. T., Ohnmacht, W., and Flower, M. J. F., 1978. Basaltic hyaloclastites from Hole 396B, DSDP Leg 46. In Dmitriev, L., Heitzler, J., et al., *Init. Repts. DSDP*, 46: Washington (U.S. Govt. Printing Office), 341–346.

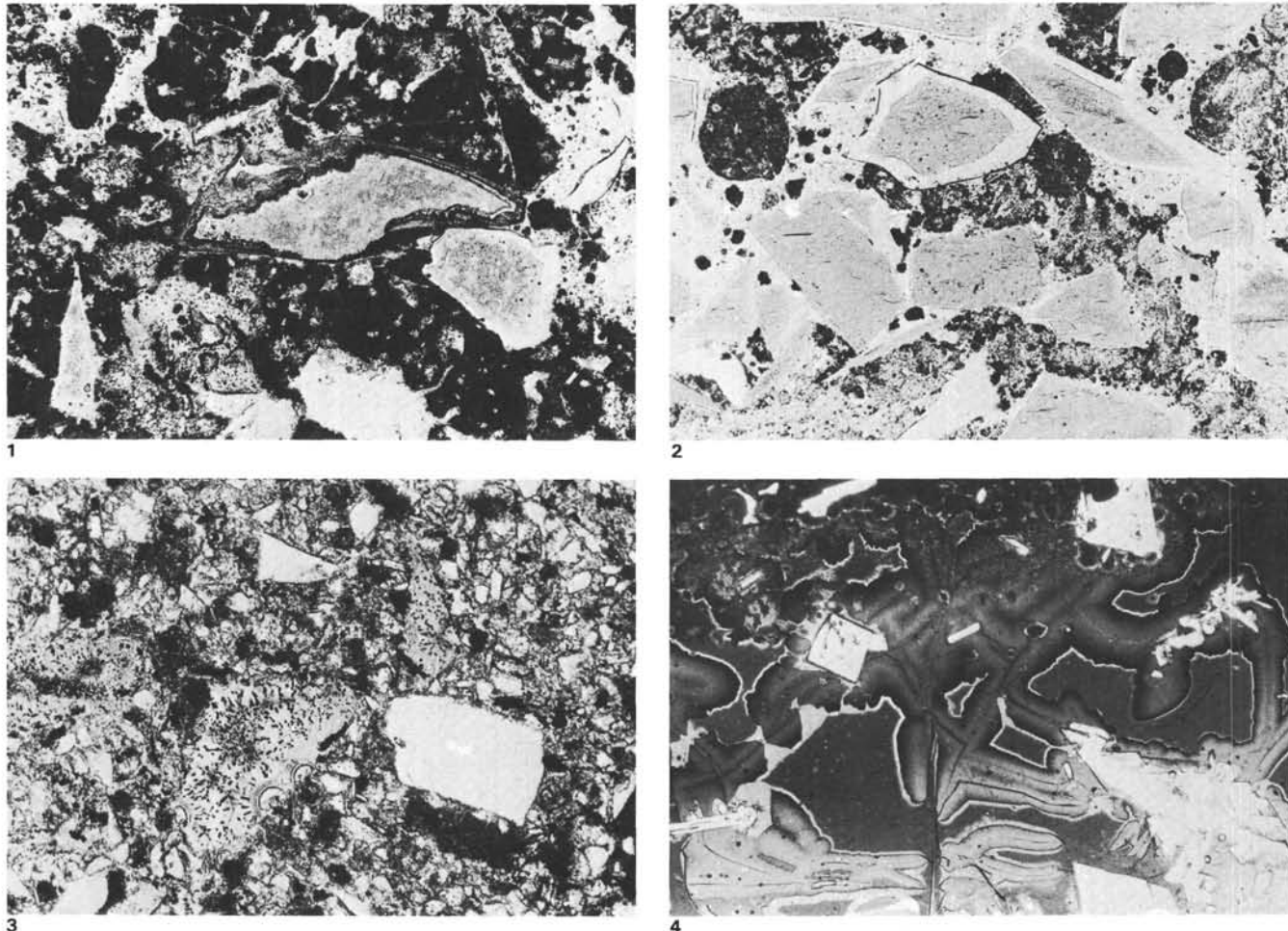


Plate 1. Tephra deposits recovered on Leg 65. 1. Marginally palagonitized shard in center of photomicrograph showing layers of "gel-palagonite" (width of photomicrograph, 2 mm), Sample 483-7-2, 11–16 cm. 2. Fresh sideromelane shards set in nonvolcanic silt and fecal pellets (note angular blocky shape of shards); former palagonite rim of some shards has been removed by grinding (width of photomicrograph, 5 mm), Sample 483-7-2, 11–16 cm. 3. Indurated hyaloclastite consisting of completely altered sideromelane shards set in a nonvolcanic matrix of silt and fine sand. The shards are now represented by light smectite, concentric banding representing successive stages of palagonitization and a dark Ti-rich(?) phase. The large plagioclase crystal (right) has also been marginally dissolved, the void being partially filled by zeolite (width of photomicrograph 5 mm), Sample 483B-8-1, 21–28 cm. 4. Photomicrograph of glass alteration at the base of a massive flow. Dark brown homogeneous areas are sideromelane, grading outward into a colorless "palagonite" rim followed, across a sharp transition, by dark through light-brown "palagonite" (width of photomicrograph, 5 mm), Sample 483B-26-1, 39–40 cm.